

WEAR BEHAVIOR OF CRYOGENICALLY TREATED AISI 420 MARTENSITIC STAINLESS STEEL

G. Prieto^{1,2(*)}, W. R. Tuckart^{1,2}

¹Tribology Group, Universidad Nacional del Sur, Bahía Blanca, Argentina.

²Consejo Nacional de Investigaciones Científicas y Técnicas, Ciudad Autónoma de Buenos Aires, Argentina.

* german.prieto@uns.edu.ar

ABSTRACT

Cryogenic treatments have been employed over the last three decades in both tool and high-alloy steels to improve wear resistance, mainly through the transformation of retained austenite and the precipitation of fine carbides. In this work the wear behavior of deep cryogenically treated (DCT), low-carbon AISI 420 martensitic stainless steel specimens has been studied with respect to that of conventionally heat treated (CHT) ones.

The tribological properties of the materials were assessed by means of ball-on-disk tests, under a range of applied normal loads in a paraffinic additive-free vaseline bath. The disks were made of AISI 420 stainless steel subjected to two different heat treatments, namely, quenched and annealed (CHT), and quenched, soaked in liquid nitrogen for 2 h and annealed (DCT). A 5 mm tungsten carbide ball was used as the counterbody. Wear behavior has been characterized by wear volume, friction coefficient measurements and analyses of worn surfaces, wear debris and subsurfaces. It was found that the wear resistance of cryogenically treated specimens showed increases ranging from 35% to 39% in comparison to the conventionally treated ones.

KEY WORDS: wear resistance, cryogenic treatments, carbides, ratchetting.

1.- INTRODUCTION

Cryogenic treatments are being increasingly used as a manufacturing technique to improve wear resistance and dimensional stability of a wide range of materials, ranging from high-alloy tool steels to non-ferrous alloys, such as copper, magnesium and aluminum alloys. This kind of treatments possess several advantages, such as its relative low cost, ease of application and volumetric effect. This latter property means that the whole volume of the workpiece exhibits a wear resistance enhancement, in comparison to superficial techniques such as plasma nitriding, electrodeposited coatings or case carburization.

One of the first systematic studies regarding the influence of cryogenic treatments over a wide range of steels was performed by Barron [1]. The results reported in his research showed that cryogenic treatments increased the wear resistance, specially in the case of tool steels. In this early work it was found that cryogenically treated stainless steels exhibited a wear resistance enhancement in the order of 10% compared to conventionally treated specimens, whereas plain carbon steel and cast iron showed no significant improvement after deep cryogenic treatment (DCT).

The application of deep cryogenic treatments is associated to the transformation of retained austenite and the precipitation of small second phase particles, such as secondary carbides [2]. In the case of the AISI 420 martensitic stainless steel, it has been found that the modification of its mechanical properties after cryogenic

treatment is mainly due to the precipitation of secondary carbides, with a smaller average diameter and a more homogeneous size distribution when compared to CHT specimens [3], whereas transformation of retained austenite had no significant effect. As stated before, the precipitation of small secondary carbides is an important phenomenon related to wear enhancement. In this sense, Meng et al. [4, 5] and Stratton et al. [6, 7] addressed this subject in their studies. They found that cryogenic treatments generate not only the precipitation of a higher amount of secondary carbides, but also a reduction of the average particle size and a homogenization of particle size distribution with regard to conventionally treated specimens. It is worth noting that the majority of the research efforts related to cryogenic treatments has been focused in high-alloy steels, in which the variety and volume fraction of alloy elements promotes the precipitation of a wider range of carbides.

Due to its usage in pumping applications related to oil industry, it is interesting to evaluate the tribological response of cryogenically treated AISI 420 stainless steel. This steel can be usually found in valves and pump rotors used for oil extraction and in refinement operations, therefore they are subjected to severe mechanical and tribological solicitations.

The tribological tests performed in this present study demonstrated that cryogenically treated specimens had a superior wear resistance with regard to conventionally heat treated ones, with improvements ranging from 35% to 39%. This behavior is attributed to the less degree of plastic deformation and sub-surface cracking found in the wear scars of cryogenically treated specimens in comparison to the conventionally treated ones.

2.- MATERIALS AND METHODS

A low-carbon, AISI 420 martensitic stainless steel has been used in the present study. Its chemical composition, shown in Table 1, was determined using a SPECTRO MAXX optical emission spectrometer. The results are shown along with the reference composition taken from ASM Metal Handbook Volume 3 [8].

Pin-on-disk tests were used for wear behavior characterization. For this purpose, AISI 420 steel disks were machined, with a diameter of 42 mm. Two groups of specimens were prepared, namely, a conventionally heat treated one (CHT), in which the disks were quenched in oil from 1030 °C and afterwards, annealed at 410 °C for 10 min with furnace cooling. The other group of disks were quenched in oil from 1030 °C and then soaked in liquid nitrogen, at an equilibrium temperature of -196,4 °C. The cooling rate was set at 0.45 °C/s and the soaking time at cryogenic temperature was of 2 h. Finally, the specimens were annealed at 410 °C for 10 min and slowly cooled inside the furnace. This latter group was identified as DCT. All specimens were polished using abrasive silicon carbide papers up to 600 grit and ultrasonically cleaned with toluene for 5 min before and after each test. A 5 mm diameter tungsten carbide ball was used as the counter-body. Roughness parameters were determined using a HOMMEL ETAMIC T-500 contact stylus profilometer prior testing, with a 4.8 mm cut-off length.

The sliding speed in all cases was 0.06 m/s, while the sliding distance was set at 500 m. The applied normal loads were 5, 10, 15, 20 and 25 N. During the test, the friction force was continuously measured and logged with a data acquisition system. Tests were performed in a low-viscosity, additive-free paraffinic vaseline bath, with a cinematic viscosity of 17 cSt at 40 °C. All the experiments were performed under ambient laboratory conditions (~25 °C, 65% relative humidity). Wear volume was

calculated following ASTM G-99 standard [9] using at least 3 valid tests for each experimental condition.

Wear surfaces were analyzed by means of an NIKON ECLIPSE LV-100 optical microscope. NIKON NIS-ELEMENTS D image processing software was used for measuring wear track width, at least at 30 different positions. SEM images and EDS measurements were also used to characterize worn surfaces and sub-surfaces, by means of a JEOL JSM-35CF scanning electron microscope, equipped with an energy dispersive X-ray spectrometer. For sub-surface examination, worn disks were cut using a slow speed cold cut saw and carefully polished until the transversal section became tangential to the wear scar. Final polishing was made with an alumina suspension (particle size: 3 μm). Afterwards, specimens were attacked using Marble reagent (10 g CuSO_4 in 50 ml HCl and 50 ml water), during 5 s in order to reveal the microstructural features.

3.- RESULTS AND DISCUSSION

Roughness measurements taken prior to tribological testing showed that average roughness (R_a) was $0.077 \text{ mm} \pm 0.003 \text{ mm}$, while maximum profile peak height (R_p) was $0.290 \text{ mm} \pm 0.034 \text{ mm}$ and R_z was $0.644 \text{ mm} \pm 0.026 \text{ mm}$.

Table 1. AISI 420 chemical composition (wt%)

	C	Cr	Si	Mn	P	S	Fe
Bar	0.177	12.83	0.55	0.76	0.05	0.017	Balance
AISI 420 Datasheet	0.15 min	12.00-14.00	1.00 max	1.00 max	0.04 max	0.03 max	Balance

Wear rate in DCT specimens was lower than CHT ones at all the applied normal loads, being the difference of 39% at 5 N, 35% at 10 N, 36% at 15 N, 37% for 20 N and 38% for 25 N. The response of both groups of materials was similar, with an increasing value of wear rate as the applied normal load was augmented. This behavior can be seen in Figure 1a, that shows the wear rate as a function of applied normal load.

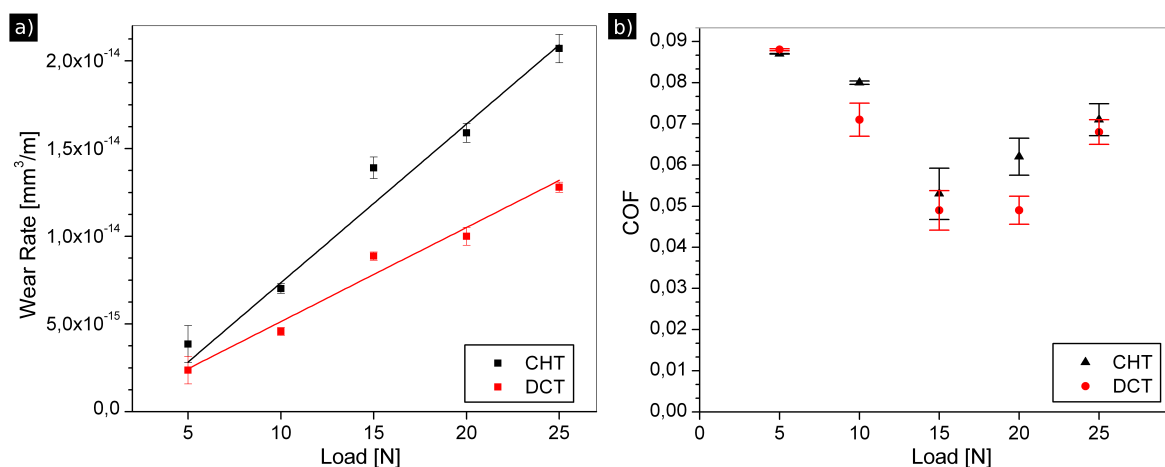


Figure 1. a) Wear rate and b) COF value as a function of the applied normal load

A wide range of wear resistance increments can be found in the literature. Barron [1] reported a 21% wear resistance increase in a cryogenically treated AISI 440

martensitic stainless steel. Das et al. [10] reported improvements ranging from 21% to 257% in a AISI D2 die steel, while Bensely et al. [11] had reported an average improvement in wear resistance of 372% when studying a cryogenically treated case carburised steel. Meng reported increases of up to 600% in [5] and between 180 and 200% in [6]. Thus it can be inferred from our results that cryogenic treatments generate a moderate improvement in the wear resistance of AISI 420 stainless steel, accounting for an average increase of 37%.

It can be seen in Figure 1b. that the COF of DCT specimens was slightly lower than the corresponding to CHT specimens. It is interesting to note that the COF values were very low for both CHT and DCT specimens, ranging between 0.05 and 0.08 in all cases. A minimum value can be observed at 15 N for both groups of specimens, this phenomenon is related to the formation of certain oxide layers. A more detailed characterization of these layers is the subject of our further studies.

The worn specimens were examined using both optical and scanning electronic microscopy. It can be seen in Figure 2 that the surface morphology of the wear scars is quite similar for CHT and DCT specimens, where both specimens developed oxide layers in the wear scar.

DCT specimens shown a more uniform oxide layer (Figure 2b), that became compacted during sliding, in contrast with the corresponding to the CHT specimens (Figure 2a), that developed a rougher surface with several patches, signaling oxide spallation.

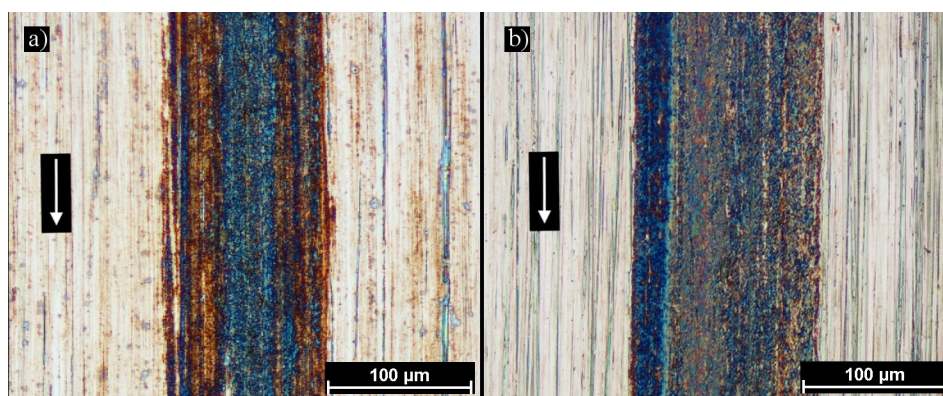


Figure 2. OM images at 500 \times of wear scars of a) CHT specimen and b) DCT specimen. 25 N of applied normal load. Arrows indicate sliding direction.

The effect of increasing the normal load is shown in Figure 3, in which not only a wear scar widening can be seen, but also a change in coloration, with a stronger presence of blueish oxides. This is associated to higher temperatures in the contact zone. At high load levels, mild adhesion and oxide layer transfer levels between the disk specimens and the counter-body were observed for both CHT and DCT specimens.

The examination of wear debris and transversal images indicates delamination wear. Suh [13] proposed that there is an accumulation of plastic shear deformation due to the surface traction induced by the sliding of a hard indenter on a soft surface. This accumulation process favors sub-superficial crack nucleation -as it can be clearly seen in Figure 5- and when the cracks reach a certain size, they generate flake-like wear debris. Some extent of oxide spallation can be appreciated in Figures 2 and 3, as oxide layers grow in thickness, they reach a critical size and break-off the surface.

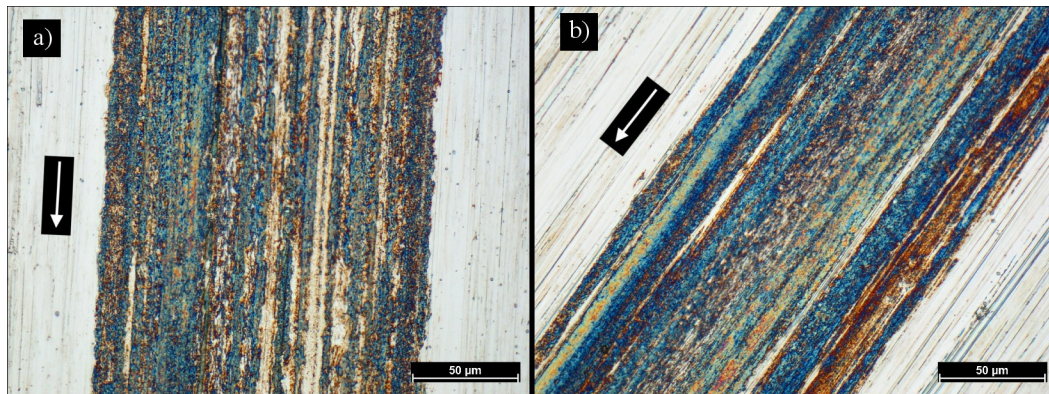


Figure 3. Wear scars OM images at 200 \times of CHT specimens at a) 15 N b) 25 N applied normal load. Arrows indicate sliding direction.

Figure 4 shows the formation of slivers along the worn surface. These superficial features are commonly associated to a ratchetting process and are expected to form under unidirectional sliding tests. These slivers grow by plastic deformation until a thin plate-like debris is formed, subsequently breaking off and detaching from the surface. In Figure 4b it can be observed that the amount and extension of slivers is less noticeable in DCT specimens. Additionally, their worn surface was more uniform compared with CHT ones.

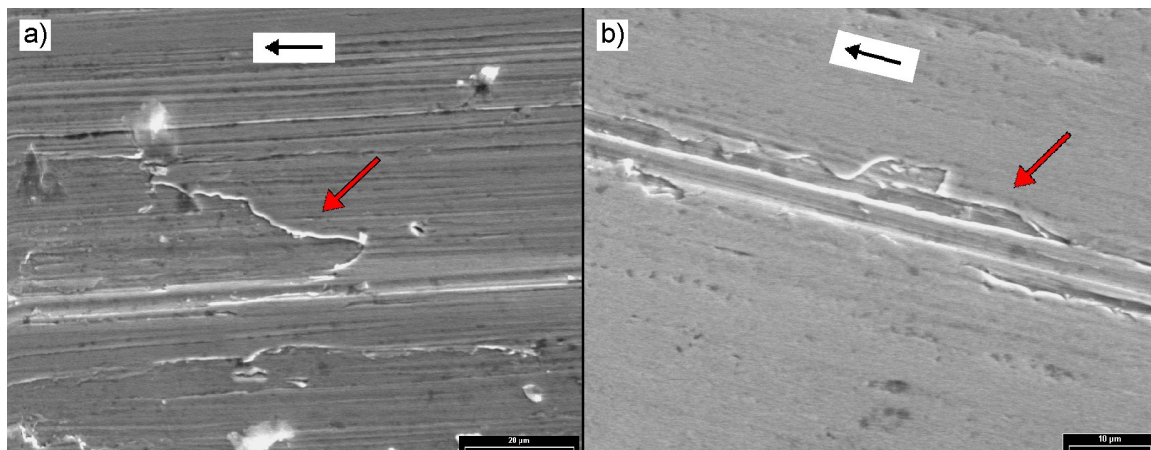


Figure 4. SEM image of worn surfaces of a) CHT specimen at 1800 \times ; b) DCT specimen at 2000 \times . The applied normal load was 25 N in both cases. Extrusion slivers (marked with red arrows) can be seen, signaling ratchetting damage. The black arrows indicate the sliding direction.

The damage beneath the surface of the wear track of a CHT specimen can be appreciated in Figure 5. The martensitic microstructure has been strained along the sliding direction, showing a fair amount of plastic deformation. DCT specimens exhibited similar characteristics. The bright zones near the surface correspond to the oxide layers. A developing sub-superficial crack can be seen in the region highlighted by the red box, this phenomenon is consistent with the ratchetting damage that is observed in Fig. 4a, thus supporting the proposition that the active wear mechanisms are a combination of ratchetting and oxide spallation.

Individual carbides can be seen near the surface layer, as well as a carbide cluster, that has also been distorted by the shear stresses developed during sliding. These results support the hypothesis that carbide distribution plays a fundamental role in the modification of the wear resistance of steel alloys. In [6] Meng et al. addressed this subject more thoroughly, reporting a reduction in the average carbide size of the same order than the registered in our specimens [4]. In that case, the volume fraction of retained austenite was below the detection limit of the x-ray diffractometer (~3%), even for the quenched and tempered condition.

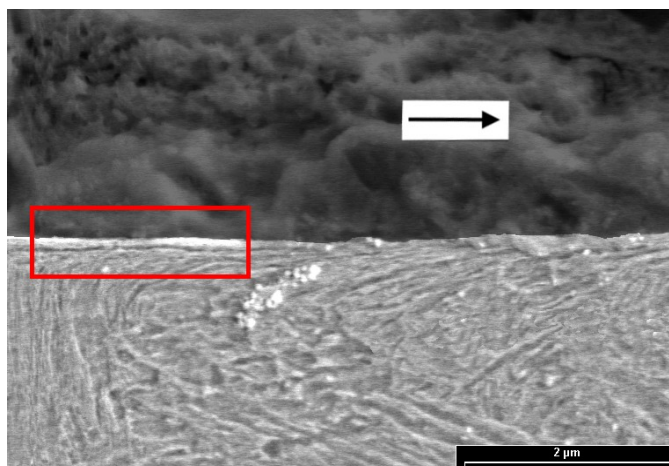


Figure 5. Cross sectional SEM image at 1800× of a CHT specimen tested at 25 N applied normal load, showing plastic deformation of martensite laths and carbide clusters along with sub-superficial cracking. The arrow indicates the sliding direction.

The main microstructural difference between CHT and DCT specimens was that the latter exhibited a higher amount of fine secondary carbides [4], with a more homogeneous size distribution. These results are in strong accordance with those reported by Meng et al. [5] while studying the precipitation of nanometric rod-like carbides in the range of 20 to 40 nm. DCT specimens exhibited a higher amount of finer η -carbides carbides, while bigger ε -carbides were found in CHT specimens. Suh also hypothesized about the influence of inclusion – matrix interfaces and their effect over crack nucleation [13], recognizing that this type of features act as stress concentrators. As a consequence, cracks can nucleate at lower stress levels in the surroundings of inclusions and second phase particles. This could explain the wear resistance improvement of cryogenically treated specimens as they had smaller carbides and more evenly dispersed in the matrix. This hypothesis have been addressed more deeply by Pandkar et al. [14] and Bhattacharyya et al. [15] while studying the effect of microstructural features, such as carbide size and distribution, in the resistance to rolling contact fatigue of bearing alloys.

5.- CONCLUSIONS

From the obtained results it can be concluded that cryogenic treatments generate a moderate increase in the wear resistance of AISI 420 martensitic stainless steel at all the tested loads. This behavior is attributed to the less plastic deformation and sub-surface cracking found in the wear scars of cryogenically treated specimens in comparison to the conventionally treated ones. Additionally, the linearity of the results indicates that the same wear mechanism was operative in all cases.

ACKNOWLEDGEMENTS

The authors appreciate the collaboration of Mr. Gustavo Montesi of the Engineering Department – UNS for his collaboration with specimens and tribometer preparation, and to the National Agency of Science and Technology Promotion for the financial assistance received (Grant code: PICT 2013-0616).

REFERENCES

- [1] Barron RF. Cryogenic treatment of metals to improve wear resistance. *Cryogenics*, 22 (1982) 409–413.
- [2] Tyshchenko AI, Theisen W, Oppenkowski A, Siebert S, Razumov ON, Skoblik AP et al. Low-temperature martensitic transformation and deep cryogenic treatment of a tool steel. *Mater. Sci. Eng. A.*, 527(26) (2010) 7027–7039.
- [3] Prieto G, Perez Ipiña JE, Tuckart WR. Cryogenic treatments on AISI 420 stainless steel: Microstructure and mechanical properties. *Mater. Sci. Eng. A.*, 605 (2014) 236–243.
- [4] Meng F, Kohsuke T, Azuma R, Sohma H. Role of eta-carbide precipitations in the wear resistance improvements of Fe-12Cr-Mo-V-1.4C tool steel by cryogenic treatment. *ISIJ Int.*, 34(2) (1994) 205–210.
- [5] Meng F, Tagashira K, Sohma H. Wear resistance and microstructure of cryogenic treated Fe-1.4Cr-1C bearing steel. *Scr. Metall. Mater.*, 31(7) (1994) 865–868.
- [6] Stratton P, Graf M. The effect of deep cold induced nano-carbides on the wear of case hardened components. *Cryogenics*, 49(7) (2009) 346–349.
- [7] Stratton P. Optimising nano-carbide precipitation in tool steels. *Mater. Sci. Eng. A.*, 449 – 451 (2007) 809–812.
- [8] Hardesty F, *Metals Handbook*, 9th ed., Handbook Committee, ASM, Metals Park, OH, USA, 1980.
- [9] ASTM Standard G99, Standard Test Method for Wear Testing with a Pin-on-Disk Apparatus, ASTM International, West Conshohocken, PA, 2010.
- [10] Das D, Dutta AK, Ray KK. Sub-zero treatments of AISI D2 steel: Part II. Wear behavior. *Mater. Sci. Eng. A.*, 527(9) (2010) 2194–2206.
- [11] Bensely A, Prabhakaran A, Mohan Lal D, Nagarajan G. Enhancing the wear resistance of case carburized steel (En 353) by cryogenic treatment. *Cryogenics*, 45(12) (2005) 747–754.
- [13] Suh, N. P. An overview of the delamination theory of wear. *Wear*, 44 (1977) 1-16.
- [14] Pandkar AS, Arakere N, Subhash G. Microstructure-sensitive accumulation of plastic strain due to ratchetting in bearing steels subject to Rolling Contact Fatigue. *Int. J. Fatigue*, 63 (2014) 191–202.
- [15] Bhattacharyya A, Subhash G, Arakere N. Evolution of subsurface plastic zone due to rolling contact fatigue of M-50 NiL case hardened bearing steel. *Int. J. Fatigue*, 59 (2014) 102–113.